International Journal of Advanced Engineering Research and Science (IJAERS)
Peer-Reviewed Journal
ISSN: 2349-6495(P) | 2456-1908(O)
Vol-9, Issue-6; Jun, 2022
Journal Home Page Available: https://ijaers.com/
Article DOI: https://dx.doi.org/10.22161/ijaers.96.8

Computer simulation of reinforced concrete columns confined with CFRP

Tiago Nobre da Silva[1], Carla Simone de Albuquerque[1], Mauro de Vasconcellos Real[1], Francisco Eudázio Suriano da Silva Júnior[2]

[1]Graduate Program in Computational Modeling, Federal University of Rio Grande, Rio Grande do Sul, Brazil
Email: nobretiago2@gmail.com
[1]Graduate Program in Computational Modeling, Federal University of Rio Grande, Rio Grande do Sul, Brazil
Email: carla19matematica@gmail.com
[1]Graduate Program in Computational Modeling, Federal University of Rio Grande, Rio Grande do Sul, Brazil
Email: mauroreal@furg.br
[2]Graduate Program in Civil Engineering, Federal University of Santa Catarina, Santa Catarina, Brazil
Email: jrsuri@outlook.com

Received: 07 May 2022,

Received in revised form: 01 Jun 2022,

Accepted: 08 Jun 2022,

Available online: 15 Jun 2022

Keywords*— *CFRP, Columns, Finite Element, Reinforced Concrete, Reinforcement

Abstract*—*Carbon Fiber Reinforced Polymer (CFRP) reinforcement of reinforced concrete (RC) columns has become increasingly common. This work presents a finite element computational model capable of representing the structural behavior of CFRP-confined square RC columns. Data and results from experimental research available in the literature are used to assess the ability of the proposed model to represent the test results. It is possible to observe that the models were able to represent, with adequate precision, the structural behavior of columns with different configurations of longitudinal reinforcement, stirrups spacing, number of CFRP layers, and type of load.

I. INTRODUCTION

Due to the aging of buildings or even the change in use of the structure, reinforcing RC structures can become the most economical and viable option to be carried out. According to Souza and Ripper [1], the reinforcement of columns is always more problematic than beams and slabs. The columns are the last elements of support of the structure before the loads reach the foundations and have to obey safety and economic criteria in any situation.

Among the existing methods, the reinforcement of columns with CFRP (Polymer Reinforced with Carbon Fiber) has become increasingly common. Saadatmanesh and Ehsani [2] state that the growth in the use of composites is mainly due to their high tensile strength, high modulus of elasticity, and excellent corrosion resistance.

This reinforcement technique in columns works due to the lateral confinement promoted by the CFRP. However, according to Carrazedo [3], confinement is only appropriately enabled with the development of microcracks at a high-stress level since the lateral deformation of concrete is very small before the beginning of microcracking. Therefore, this reinforcement technique is classified as a passive form of confinement.

Several experimental works in the literature address the reinforcement of RC columns with CFRP wrap. However, elaborating all the procedures of experimental research can become onerous. Therefore, using computational methods

capable of representing the structural behavior of columns can be considered an interesting alternative.

Computer simulations of concrete structures, for the most part, are with the finite element method (FEM). Real *et al.* [4] explain that in the FEM, the structure is divided into small elements that are linked together through nodal points. This method solution is determined through the displacements, which are the unknowns of the problem. The internal stresses of the element and the reactions at the supports are calculated from these displacements.

In Brazil, the Brazilian Standard (NBR) that deals with reinforced concrete elements' design and structural behavior is the NBR 6118 [5]. However, this standard still does not provide prescriptions regarding the design and construction procedures of CFRP reinforcements. Therefore, conducting research in this area is essential in the national context.

Most Brazilian research on carbon fiber reinforced structures is based on international normative recommendations. Therefore, this research aims to demonstrate the computational simulation of RC columns reinforced with CFRP to contribute to the scientific community as a technical asset for future Brazilian standardization of this reinforcement technique.

II. METHOD

This work was carried out using the experimental results of research by Wang *et al.* [6], Atheer *et al.* [7], and Souza [8] as a reference in terms of comparison to validate the computational model used. The computational modeling was performed using the Ansys Workbench 17.1 software, which performs simulations using the finite element method.

2.1 – Finite element analysis (FEA)

The SOLID65 element was used to represent the concrete. According to ANSYS [9], SOLID65 is a 3D element, with eight nodes, with a material model capable of cracking under tension and failure by crushing in compression and having the ability to suffer creeping. This element supports up to four different materials for each finite element, with one being the principal material and the reinforcement bars distributed inside the element volume, being ideal for representing the reinforced concrete

The linear element LINK180 represented the longitudinal reinforcement and stirrups of the columns. According to ANSYS [9], the LINK180 element can be used to model cables and bars and has two nodes with three degrees of freedom at each node. This element resists only axial forces and considers the steel reinforcement's elasticity, plasticity, and creep characteristics. In addition, its cross-section can increase or decrease when the element is subjected to compression or tension.

The SHELL 181 element was used for the CFRP, which is capable of considering the change in the thickness of the CFRP in nonlinear analysis, a characteristic that makes it able to evaluate the internal stress distribution during the study of the structure where it is associated. According to ANSYS [9], it is a four-node element with six degrees of freedom at each node (translations in the x, y, and z directions and rotations about the x, y, and z axes). Fig. 1 represents the elements used.

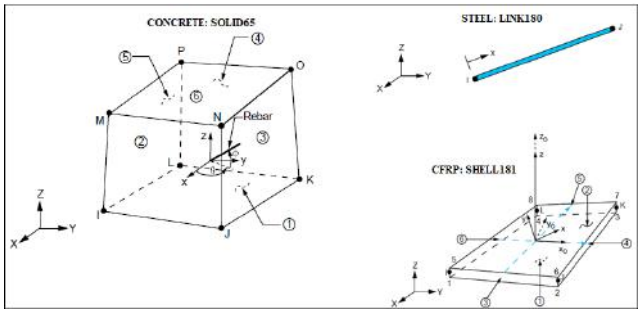

Fig. 1- Types of the elements used in the FEA

The failure mode of the SOLID65 element used is based on the criterion of William and Warnke [10]. These equations consider both the crushing and cracking failure of the concrete. Poisson's coefficient was 0.2 in all columns, while the hydrostatic, shear transfer coefficients for closed cracks and shear transfer coefficients for open cracks were defined as 1.0, 0.3, and 1.0, respectively.

A discrete model was used to idealize the stiffness of the steel. According to Ayala [11], it is a model that requires that the nodes of the SOLID65 and LINK180 elements coincide. This element combination is the ideal model for the constitutive equations of William and Warnke [10].

A mesh convergence test was performed to determine the best mesh configuration. For the columns of Wang *et al.* [6], meshes of 7,625 mm were used in x and y directions for concrete, while for CFRP, a mesh of 20 mm was employed. In the columns of Atheer *et al.* [7], meshes of 7.5 mm were adopted in x and y directions for concrete, and a mesh of 12.5 mm was defined for CFRP. Finally, in the columns of Souza [8], were used meshes of 6.25 mm in the x-direction and 28.52 mm in the y-direction for concrete and a mesh of 12.5 mm was defined for CFRP. The meshes used are shown in Fig. 2 - 4.

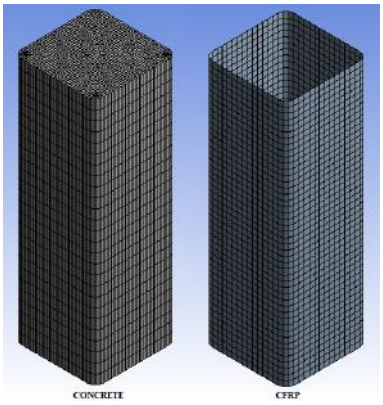

Fig. 2 – Mesh of the columns by Wang et al. [6]

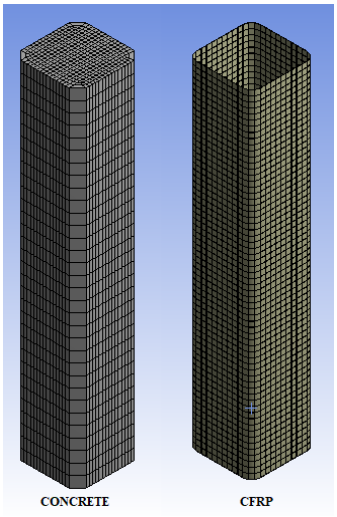

Fig. 3 – Mesh of the columns by Atheer et al. [7]

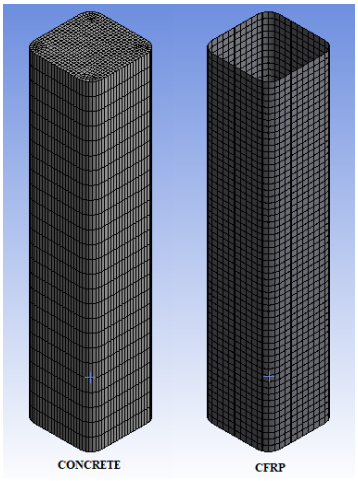

Fig. 4 – Mesh of the columns by Souza [8]

The analysis was performed considering the lower face of the columns fixed in the Y direction to represent the models' reaction. In contrast, the upper face was considered free to move. A displacement in the Y direction was applied in this region to represent the load action. This action was subdivided into "substeps" adjusted for each model. Like the mesh convergence test, the appropriate number of "substeps" depends on tests and the geometry of each model.

The Newton-Raphson method, which was used in this analysis, is one of the ways used by ANSYS [9] to solve nonlinear analyses. According to Pivatto [12], this method approaches the equilibrium trajectory of the structure by its tangents until reaching convergence. The displacement increments were applied until the column load capacity had been exceeded.

III. RESULTS AND DISCUSSION

3.1 – Experiments by Wang *et al.* [6]

The experimental work by Wang *et al.* was carried out to study the influence of the variation of the stirrups spacing and the number of layers CFRP in columns of larger dimensions than are generally found in the literature. The authors tested 34 columns with two identical specimens; there were 17 column configurations. One column of each format was tested for a monotonic load, and the other was tested for a cyclic load. Fig. 5 presents the dimensions of the columns and the details of the longitudinal reinforcement and stirrups.

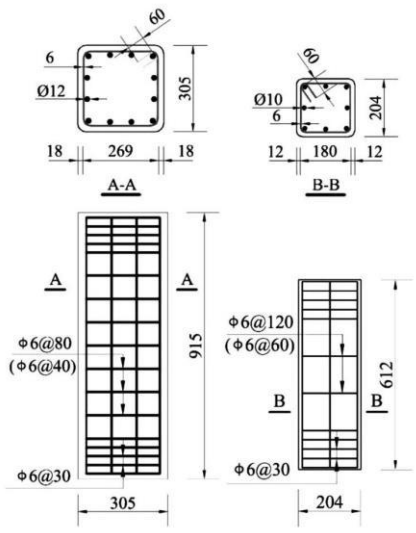

Fig. 5 – Specimen dimensions and reinforcement details of the columns by Wang et al. [6]

Table 1 – Characteristics of the materials used by Wang et al. [6]

Material	Diameter/thickness (mm)	Yield/peak strength (MPa)	Ultimate strength (MPa)	Elastic Modulus (MPa)
Longitudinal steel	10	312	484	200,000
	12	340	520	200,000
Stirrupssteel	6	397	623	200,000
CFRP wrap	0.167	-	4,340	240,000

The models are characterized as follows: The letters S1 and S2 represent the dimension of the analyzed cross-section, and the letter H represents the stirrup rate used, which can be 0 for simple concrete, 1 or 2 for a stirrup steel rate of 0.5% or 1% respectively. The letter L represents the number of CFRP layers, which can vary from 0 to 3 layers, and finally, the letter M represents the type of load used, which would be monotonic. Fig. 5 illustrates the dimensions of the tested columns and the reinforcement details. For example, the model S1H1L3M has a square cross-section of 305 mm, a stirrup steel rate of 0.5%, 3 layers of CFRP, and has been subjected to a monotonic load.

The columns received a rounding of the corners to mitigate the effects of stress concentration at the corners. It was used a rounding with a radius of 30 mm for the S1 specimens and 20 mm for the S2 specimens, keeping a ratio of twice the rounding radius per cross-section side at 0.2 so that the two models receive the same influence. The compressive strength of the concrete was 25.5 MPa on the day of the tests.

The stress was obtained by dividing the maximum load by the cross-sectional area as in the experimental results. The deformation was calculated by the ratio between the axial displacement and the height of the analyzed column. For the simulation of the columns by Wang *et al.*, axial displacements on the Y-axis were applied to the upper face of the columns. This displacement was subdivided into 200 substeps.

In terms of comparison, only the results of simulations performed with monotonic loads, i.e., continuous loading, were used. On the other hand, cyclic loads are variable loads, i.e., successive loading and unloading until the element under study fails. Furthermore, the authors did not find significant differences between the results obtained between the different types of loading. Table 2 demonstrates the comparison between experimental and computational results.

The authors reported that the confinement distribution of the CFRP was not uniform around the perimeter of the columns. The CFRP was not efficient in confining the concrete in the region in the middle of the lateral face of the columns. On the contrary, the corners were responsible for promoting the observed confinement. Therefore, the mean strain value obtained overestimated the failure stress and the effectiveness of the confinement of the CFRP. Wang *et al.* [6] concluded that the corners were the most critical points and that the CFRP strain efficiency factor was about 0.4 for the larger columns (S1) and 0.6 for the smaller columns (S2).

As in the experiments by Wang *et al.* [6], the computer models showed a more significant deformation in the middle of the lateral faces of the CFRP. Furthermore, the models with a smaller cross-section presented a greater lateral deformation when compared to the models with a larger cross-section, which is in line with the results given by Wang *et al.* [6]. Figs. 6 – 8 represent the strain on CFRP of the larger (S1) and smaller (S2) section models.

The other columns showed the same strain distribution pattern in Figures 6 - 8. Wang et al. [6] reported that the models suddenly failed in the mid-height region regarding the failure mode. Furthermore, the RC columns also showed buckling in the longitudinal reinforcement bars between the stirrups, and the concrete had been severely crushed. Fig. 9 represents the stress in the longitudinal steels and stirrups of the computational models S1H1L3M and S2H2L2M.

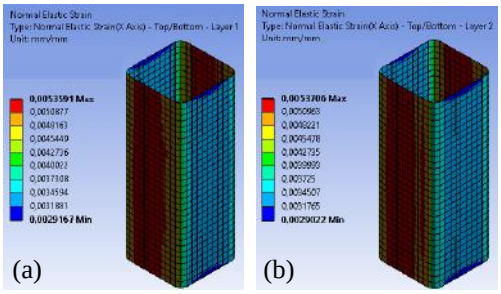

Fig. 6 – Lateral strain S1H0L2M (a) 1° layer (b) 2° layer

Table 2 – Comparison between the results of Wang et al. [6] and the proposed model

Specimen	Experimental		Computational		Variation between stress
	Axial strain (mm/mm)	Axial stress (MPa)	Axial strain (mm/mm)	Axial stress (MPa)	
S1H1L0M	0.00373	32.10	0.00241	32.79	+2.15%
S1H2L0M	0.00412	34.70	0.00249	34.77	+0.20%
S1H0L1M	0.00313	29.40	0.01090	28.60	-2.72%
S1H0L2M	0.00393	32.30	0.01311	29.73	-7.96%
S1H1L1M	0.00428	35.10	0.00459	36.43	+3.79%
S1H1L2M	0.00434	34.90	0.00361	36.70	+5.16%
S1H1L3M	0.00428	36.90	0.00448	37.60	+1.90%
S1H2L2M	0.00416	35.50	0.00426	37.50	+5.60%
S1H2L3M	0.00529	37.20	0.00535	38.50	+3.50%
S2H1L0M	0.00364	29.90	0.00359	30.24	+1.14%
S2H2L0M	0.00406	32.50	0.00327	32.89	+1.20%
S2H0L1M	0.00391	28.70	0.00817	28.69	-0.25%
S2H0L2M	0.02287	31.40	0.01307	31.98	+1.85%
S2H1L1M	0.00704	35.50	0.00653	35.00	-1.41%
S2H1L2M	0.03588	40.00	0.01471	39.996	-0.01%
S2H2L1M	0.00465	33.00	0.00474	34.77	+5.36%
S2H2L2M	0.04230	40.80	0.01634	40.76	-0.10%

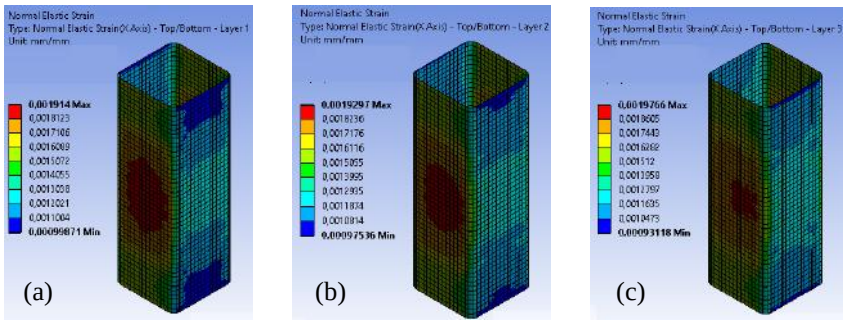

Fig. 7 – Lateral strain S1H1L3M (a) 1° layer (b) 2° layer (c) 3° layer

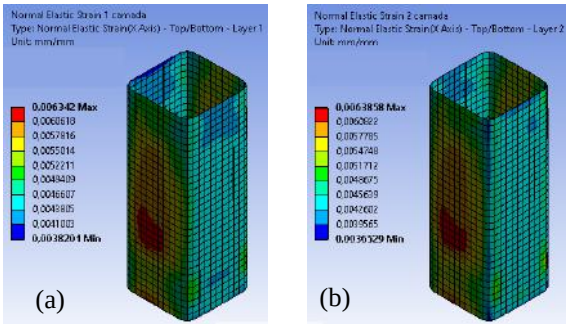

Fig. 8 – Lateral strain S1H1L3M (a) 1°layer (b) 2° layer

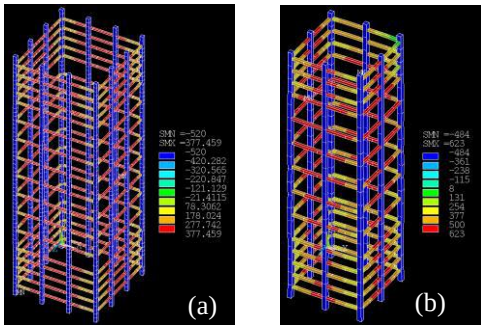

Fig. 9– Stress in the steels (a) S1H1L3M(b) S2H2L2M

As seen in Fig. 9, the longitudinal steels reached the rupture stress specified in Table 1, presenting the same failure characteristics as the RC columns tested by Wang *et al.* [6]. In addition, the authors reported that some of the columns with the largest section (S1) showed post-peak softening, which can also be observed in models S1H1L1M and S1H1L2M in the stress-strain curves of Fig. 10. In addition, the smaller section models (S2) showed an upward behavior, as can be observed in the S2H1L2M and S2H2L2M models, which was also reported by Wang *et al.* [6] in their experiment.

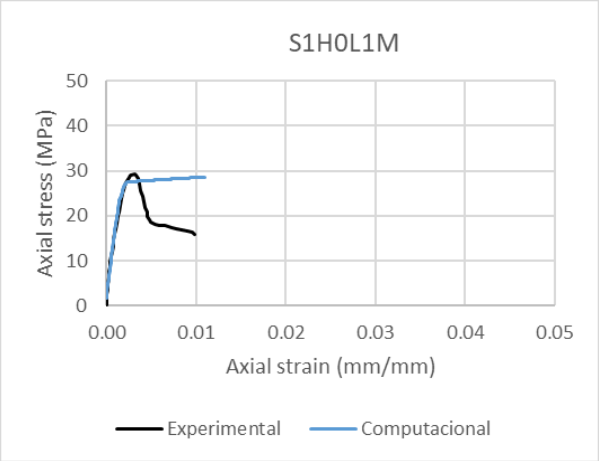

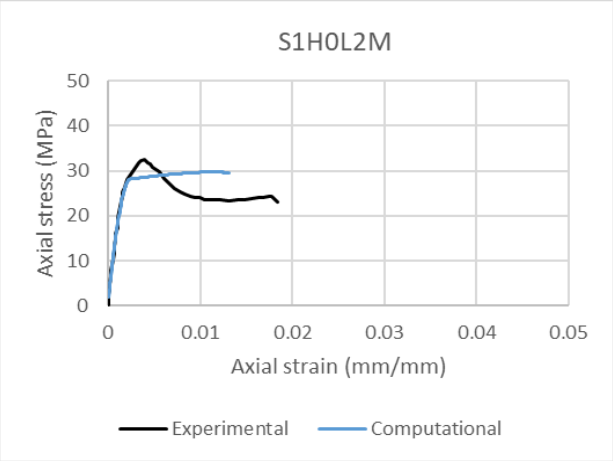

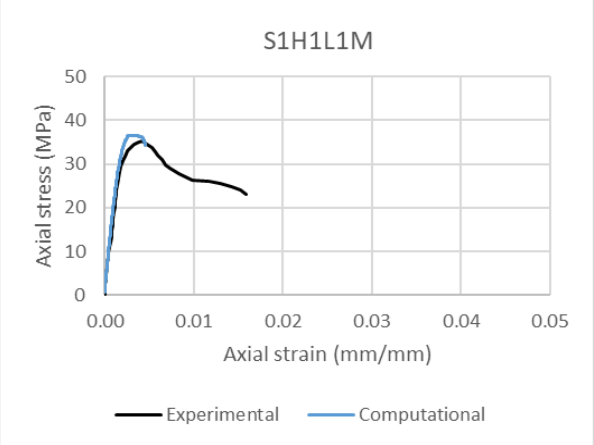

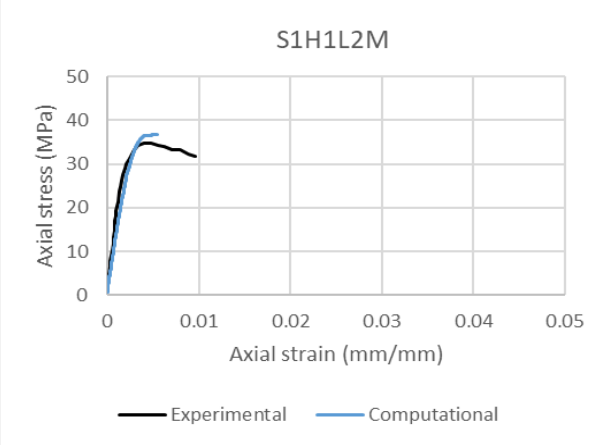

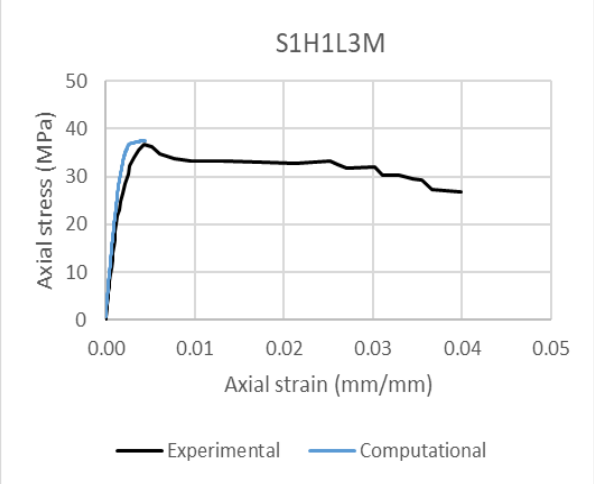

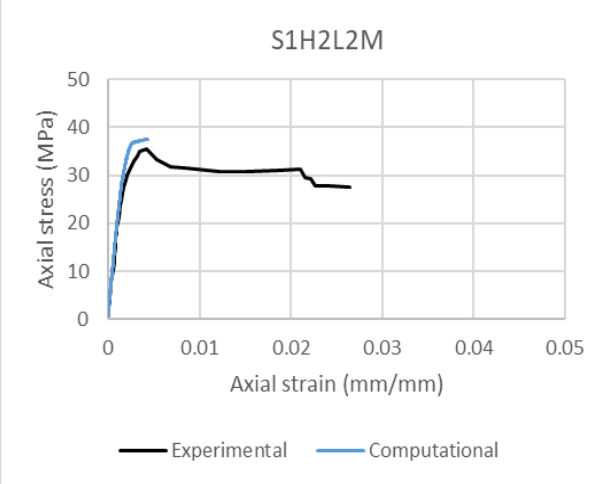

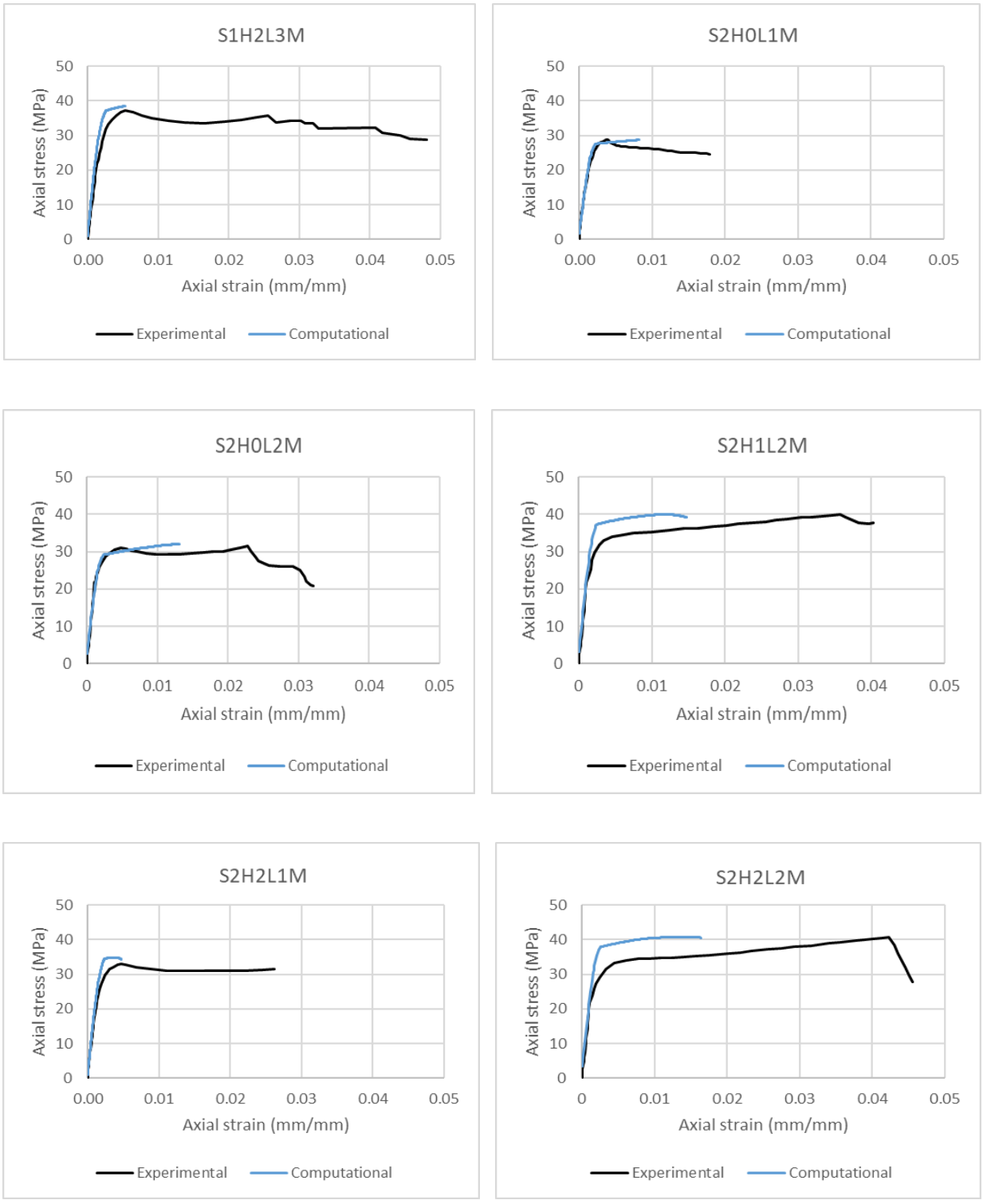

Fig. 10 – Stress-strain graphs of the computational model for the columns of Wang et al. [6]

3.2 – Experiments by Atheer *et al.* [7]

Table 3 – Characteristics of the columns by Atheer et al. [7]

Specimen	Section (mm)	Height (mm)	Longitudinal steel (mm)	Stirrups (mm)	N° CFRP wrap	Eccentricity (mm)
SF0	150 x 150	800	4 Ø 12	Ø6 c/50	2	0
SF20	150 x 150	800	4 Ø 12	Ø6 c/50	2	20
SF40	150 x 150	800	4 Ø 12	Ø6 c/50	2	40

The authors carried out an experimental study proposing a new form of reinforcement. For this, experimental simulations of CFRP-confined square RC columns were carried out to serve as a benchmark. Subsequently, circularization by concrete based on reactive powder was performed in models identical to the square ones, increasing the cross-section and changing the shape of the section of the column studied.

For the simulations, only the reference specimens were selected, that is, the CFRP-confined square models without performing the circularization, which were subjected to concentric and eccentric loads. In addition, all the columns have the same configuration, differing only by the eccentricity used. The characteristics of these columns can be seen in Fig.11.

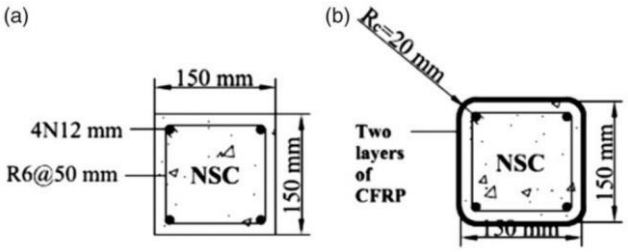

Fig. 11 – Cross-section of columns (a) S and (b) SF (Atheer et al. [7])

For the columns by Atheer *et al.* [7], the displacement applied to the upper face was subdivided into 75 substeps for model convergence. The corners received a rounding radius of 20 mm to alleviate the stress concentration in this region. Table 3 presents the details of the columns tested by Atheer *et al.* [7], while Table 4 presents the characteristics of the materials used.

Table 4 – Characteristics of the materials used by Atheer et al. [7]

Material	Average compressive (MPa)	Ultimate strength (MPa)	Elastic Modulus (GPa)	Average tensile (MPa)	Ultimate strain (%)
Concrete	25	-	-	-	-
Longitudinal steel	-	634	-	-	-
Stirrups steel	-	613	-	-	-
CFRP wrap	-	-	291	2,668	2.47

It was reported in the research that the CFRP-confined model subjected to concentric load (SF0) failed due to fragmentation of the cover due to stress concentration near the corners in the mid-height region. Fig. 12(a) shows these stress concentrations. In addition, it was reported that the longitudinal reinforcement bars buckled, as shown in Fig. 12(b).

In the specimen subjected to an eccentric load of 20 mm (SF20), fragmentation of the cover on the compression side was observed due to stress concentration. The buckling of the reinforcement bars on the compression side of the column was also observed. Figs. 13 (a) and (b) illustrate the stresses on concrete and steel reinforcements. In addition, there were cracks between the CFRP strips on the tensioned side with CFRP rupture on the compression side.

The failure mode of the model subjected to 40 mm eccentricity (SF40) was similar to that of the SF20 model,

showing fragmentation of the concrete on the compression side and cracks between the CFRP strips on the tensioned side. Fig. 14 illustrates the stresses in concrete and reinforcement steel bars.

The summary of the simulation results can be seen in Table 5, where the maximum load of the computational models is compared to the results obtained by Atheer *et al.* [7].

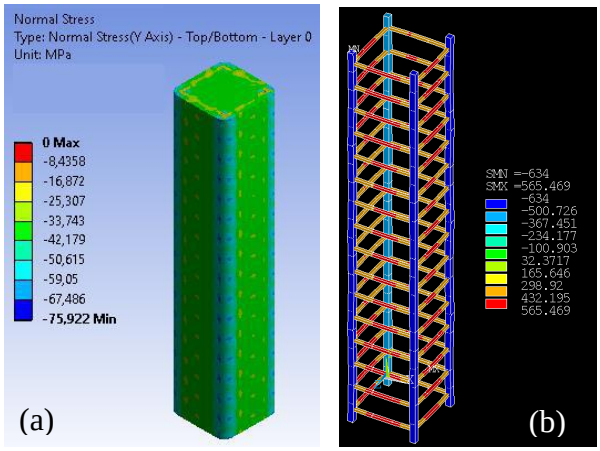

Fig. 12 – SF0 (a) stress in the concrete (b) stress in the steel reinforcements

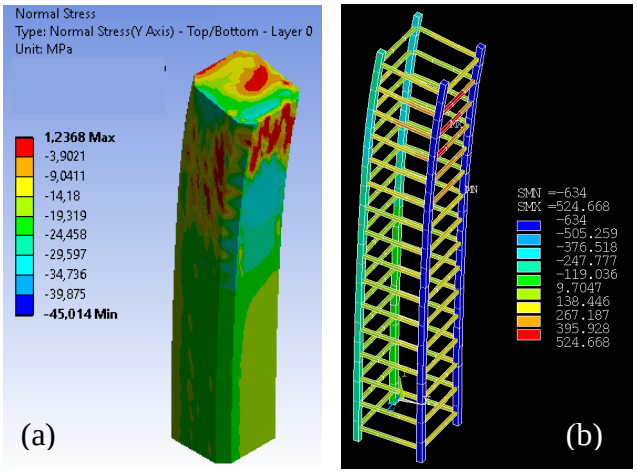

Fig. 13 – SF20 (a) stress in the concrete (b) stress in the steel reinforcements

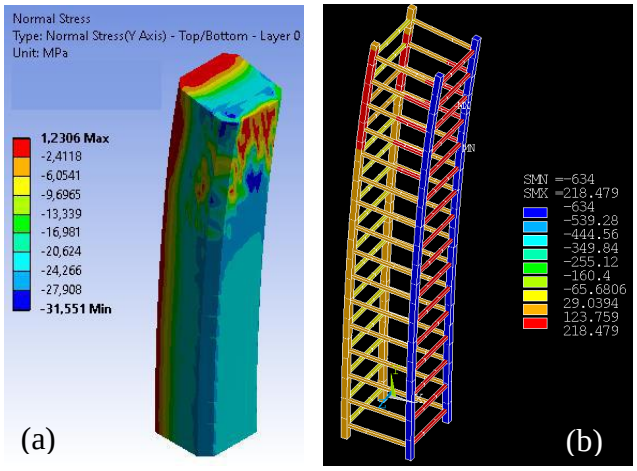

Fig. 14 – SF40 (a) stress in the concrete (b) stress in the steel reinforcements

Table 5 - Comparison between the results of Atheer et al. [7] and the proposed model

Specimen	Experimental		Computational		Variation between axial forces
	Axial displacement (mm)	Axial force (kN)	Axial displacement (mm)	Axial force (kN)	
SF0	30.50	1,462	30.00	1,466.2	+0.29%
SF20	9.10	650	3.03	670.11	+3.09%
SF40	8.9	429	2.70	462.69	+7.85 %

3.3 – Experiments by Souza [8]

Table 6 - Characteristics of Souza's [8] columns

Specimen	Section (mm)	Height (mm)	Longitudinal steel (mm)	Average compressive (MPa)	Nº CFRP wrap
G1	150 x 150	713	4 Ø 10	41.2	-
G2	150 x 150	713	4 Ø 10	23.0	-
G3	150 x 150	713	4 Ø 12.5 + 4 Ø 16	41.2	-
G1R	150 x 150	713	4 Ø 10	41.2	1
G2R	150 x 150	713	4 Ø 10	23.0	1
G3R	150 x 150	713	4 Ø 12.5 + 4 Ø 16	23.0	1

In his doctoral thesis, Souza [8] carried out experimental tests of 6 columns, being 3 CFRP-confined. The columns had the same geometric characteristics, varying only the longitudinal reinforcement steel rate and the compressive strength of the concrete. The characteristics of the columns can be seen in Table 6.

In the G3R model, the author used concrete with lower strength than his reference model to simulate a situation in which the column had a bearing capacity lower than the designed one. This situation can be found in structures of very advanced ages. Table 7 shows the characteristics of the other materials used in Souza's experiment [8].

For the columns by Souza [8], the displacement applied to the upper face was subdivided into 50 substeps for model convergence. The corners received a rounding radius of 25 mm to alleviate the stress concentration in this region.

Table 7 - Characteristics of the materials used by Souza [8]

Material	Ultimate strength (MPa)	Elastic Modulus (GPa)	Average tensile (MPa)	Ultimate strain (%)
Longitudinal steel	615	-	-	-
Hoop steel	797	-	-	-
CFRP wrap	-	231	4,205	1.8

It was reported by Souza [8] that the failure mode of the unreinforced models occurred initially in the cover region. Later there was the crushing of the concrete core, with buckling of the longitudinal steel bars. The models CFRP-confined showed rupture of the concrete core but without showing fracture of the CFRP.

The computer models showed similar behavior. The CFRP did not reach its maximum tensile capacity in any of the models (Fig. 15). The distribution of compressive stresses (Fig. 16) was also shown to be similar to the reports by Souza [8]. Therefore, the computational model failure also occurred due to the crushing of the concrete core of the column. Table 8 combines the experimental and computational simulation results, comparing the results obtained.

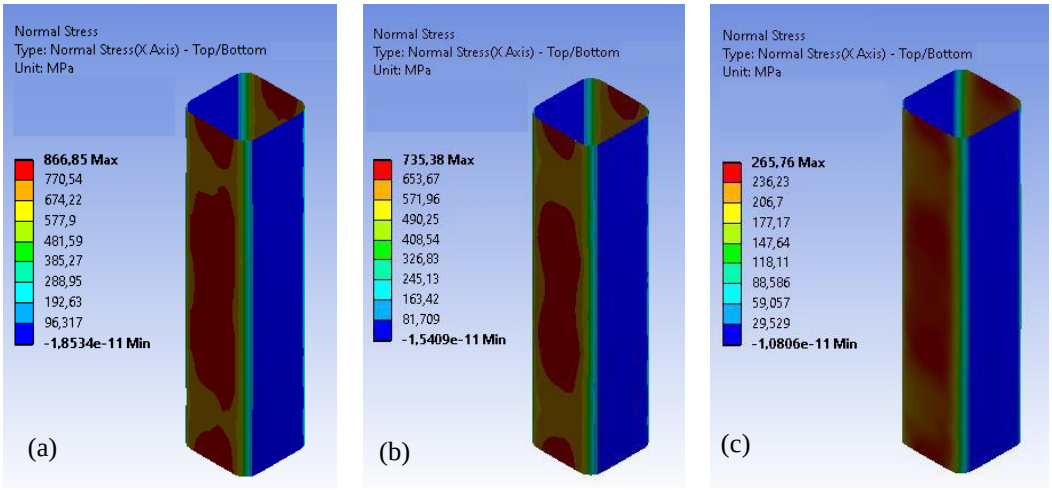

Fig. 15 – Stress in the CFRP (a) G1R (b) G2R (c) G3R

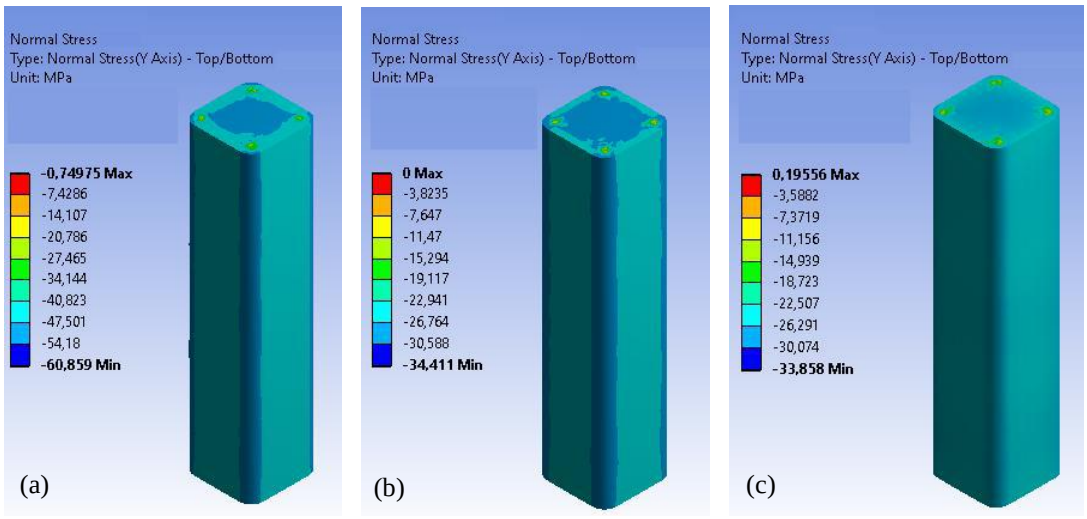

Fig. 16 – Stress in the concrete (a) G1R (b) G2R (c) G3R

Table 8 - Comparison between Souza's [8] results and the proposed model computational

Specimen	Experimental		Computational		Variation between axial forces
	Axial strain (mm/mm)	Axial Force (kN)	Axial strain (mm/mm)	Axial force (kN)	
G1	0.002423	1013	0.002104	1042.3	+ 2.89%
G2	0.001852	613	0.002524	600.4	- 2.05%
G3	0.002061	1444	0.002384	1377.9	- 4.58%
G1R	0.004600	1417	0.008415	1324.2	- 6.55%
G2R	0.005586	927	0.007010	861.26	- 7.09%
G3R	0.005653	1303	0.004909	1401.3	+ 7.54%

IV. CONCLUSION

The proposed computational model demonstrated satisfactory performance. It showed good behavior in the stress-strain graphs compared to the columns of Wang *et al.* [6]. Still, on the columns of Wang *et al.* [6], it presented good agreement in the ascending branch of the models of smaller cross-sections and the post-peak softening of some models of the larger section.

In the Atheer *et al.* [7] columns, the simulation presented maximum loads close to the experimental results, mainly in the concentric load model. However, it showed a different axial displacement in the models with eccentric loads.

Finally, in the columns tested by Souza [8], the model also had satisfactory results, demonstrating that the high rate of longitudinal steel of the G3R column reduced the lateral expansion of the column, which reduced the contribution of the CFRP in the final axial capacity of the column.

ACKNOWLEDGEMENTS

The authors would like to thank the Coordination for the Improvement of Higher Education Personnel (CAPES) and the National Council for Scientific and Technological Development (CNPq) for the financial support in developing this study.

REFERENCES

[1] SOUZA, V. C. DE; RIPPER, T. Patologia, recuperação e reforço de estruturas de concreto. São Paulo: PINI, 1998.

[2] SAADATMANESH, H. ; EHSANI, M.R. (1994). Strength and ductility of concrete columns externally reinforced with fiber composite straps. ACI Structural Journal, v. 91, p.434-447.

[3] CARRAZEDO, R. (2002). Mecanismos de confinamento e suas implicações no reforço de pilares de concreto por encamisamento com compósitos de fibras de carbono. São Carlos, 2002. 173p. Dissertação (mestrado) – Escola de Engenharia de São Carlos, Universidade de São Paulo.

[4] REAL, M. DE V, FILHO, A. C., & MAESTRINI, S. R. (2003). Response variability in reinforced concrete structures with uncertain geometrical and material properties. Nuclear Engineering and Design, 226(3), 205–220. doi:10.1016/s0029-5493(03)00110-9.

[5] ASSOCIAÇÃO BRASILEIRA DE NORMAS TÉCNICAS. Projeto de estruturas de concreto – Procedimento (NBR 6118). 2014.

[6] WANG, ZHEN & WANG, DAIYU & SMITH, SCOTT & ASCE, M & LU, DA-GANG. (2012). CFRP-confined square RC columns. I: Experimental investigation. Journal of Composites for Construction. 16. 10.1061/(ASCE)CC.1943-5614.0000245.

[7] ATHEER H. M. ALGBURI, M. NEAZ SHEIKH & MUHAMMAD N. S. HADI (2019) New technique for strengthening square-reinforced concrete columns by the circularisation with reactive powder concrete and wrapping with fibre-reinforced polymer, Structure and Infrastructure Engineering, 15:10, 1392-1403, DOI: 10.1080/15732479.2019.1623269.

[8] SOUZA, A. V. L. Reforço de pilares curtos de concreto armado de seção quadrada com mantas de polímero reforçado com fibras de carbono, 2001. Dissertação de Mestrado, Brasília, DF, Brasil. Universidade de Brasília-UNB.

[9] ANSYS. ANSYS Mechanical User's Guide. 2017.

[10] WILLIAM, K. J. AND WARNKE, E. P. Constitutive Model for the Triaxial Behavior of Concrete. Proceedings, International Association for Bridge and Structural Engineering, 19(1) (1975), ISMES, Bergamo, Italy, pp. 174.

[11] AYALA, I. C. A. Customização do software ANSYS para análise de lajes de concreto protendido pelo método dos elementos finitos. Dissertação (mestrado). Universidade Federal do Rio Grande do Sul, Porto Alegre, 2017.

[12] PIVATTO, A. B. Análise experimental e computacional de vigas biapoiadas de concreto armado reforçadas com CRFC, 2017. Dissertação de Mestrado, Curitiba, PR, Brasil. Universidade Tecnológica Federal do Paraná – UTFPR.